Partial volume effect correction in SPECT for striatal uptake measurements in patients with neurodegenerative diseases: impact upon patient classification

Marine Soret[1, 2], Pierre Malick Koulibaly[3], Jacques Darcourt[3], Irène Buvat[1]

[1] UMR 678 INSERM - UPMC, 91 Boulevard de l'Hôpital, CHU Pitié-Salpêtrière, 75634 Paris, Cedex 13, France
[2] Nuclear Medicine Department, HIA Val-de-Grâce, Paris, France
[3] Nuclear Medicine Department, Centre Antoine Lacassagne, TIRO CEA – Université de Nice-Sophia Antipolis, Nice, France

© Springer-Verlag 2006

Abstract. *Purpose:* In single-photon emission computed tomography (SPECT) of the dopaminergic system, measurements of striatal uptake are useful for diagnosis and patient follow-up but are strongly biased by the partial volume effect (PVE). We studied whether PVE correction might improve patient classification based on binding potential (BP) measurements.
Methods: Patients with a probable diagnosis of dementia with Lewy bodies (DLB, 10 patients) or Alzheimer's disease (AD, 13 patients) were studied by ^{123}I-FP-CIT SPECT. SPECT images were reconstructed with and without PVE correction. Each patient SPECT scan was also simulated to obtain SPECT data whose characteristics were fully known. In addition, 17 SPECT scans were simulated with striatal uptake values mimicking pre-symptomatic cases of DLB.
Results: Without PVE correction, mean putamen BP values were 2.9±0.4 and 0.9±0.2 for AD and DLB patients respectively, while with PVE correction, they were 8.6±1.5 and 1.9±0.5 respectively. All patients were properly identified as having AD or DLB when considering mean putamen BP measured on their real or simulated SPECT scan, with and without PVE correction. All 30 simulations mimicking pre-symptomatic DLB and AD patients were accurately classified with PVE correction, but without PVE correction 15 mean putamen BP values were in a range where AD and DLB could not be distinguished.
Conclusion: We conclude that putamen BP values measured without PVE correction can be used to differentiate probable DLB and AD due to the already severe reduction in dopamine transporter levels. PVE correction appeared useful for accurate differential diagnosis between AD and pre-symptomatic DLB.

Keywords: Brain – SPECT – Dopamine transporter – Lewy body disease – Image processing

Introduction

In single-photon emission computed tomography (SPECT) imaging of the dopaminergic system, most radiopharmaceuticals appropriate for studying the presynaptic transporter binding or the postsynaptic dopamine D_2 receptor status are labelled with ^{123}I. Common indications are early diagnosis of Parkinson's disease [1–3] and evaluation of parkinsonian syndromes [4–7]. A more recent application is the differential diagnosis between dementia with Lewy bodies (DLB) and Alzheimer's disease (AD) in demented patients. DLB is the second most common type of degenerative dementia in the elderly. Clinical diagnosis is currently based on the Consortium on DLB consensus clinical criteria [8] but definite diagnosis requires autopsy. The aforementioned clinical criteria have a high sensitivity but suffer from lack of specificity [9], AD being the most common misdiagnosis. It was recently demonstrated that FP-CIT SPECT is useful for differentiating between AD and DLB, with a significant reduction of dopamine transporters in DLB when compared with AD [10–13]. A sensitivity of 78%, a specificity of 94% and a positive predictive value of 89% have been reported for the differential diagnosis between AD and DLB based on the measurement of FP-CIT uptake [10].

Marine Soret (✉)
UMR 678 INSERM - UPMC,
91 Boulevard de l'Hôpital,
CHU Pitié-Salpêtrière,
75634 Paris, Cedex 13, France
e-mail: soret@imed.jussieu.fr
Tel.: +33-1-53828419, Fax: +33-1-53828448

Visual interpretation of the SPECT images can be considered as sufficient in many diagnostic situations. However, semi-quantification is highly recommended using, for instance, a measure of the specific binding potential (BP) of striatal sub-regions [6, 14]. A quantitative approach becomes even more important in promising indications such as the assessment of disease progression [15] and the monitoring of neuroprotective treatments [16]. The value of attenuation and scatter corrections for improving the accuracy of quantitative measurements has already been demonstrated [17, 18]. Even with these corrections, BP values remain underestimated by about 50% when measured within anatomical volumes of interest, because of the partial volume effect (PVE) [19, 20]. Anatomically guided partial volume correction combined with attenuation and scatter corrections reduced the bias in BP estimates to about 10% [19].

Moreover, it is known that when parkinsonian symptoms appear, the dopamine transporter is already reduced by 50% or more [21]. A reduction of 64% in the dopamine transporter was necessary to induce a parkinsonian state in a non-human primate model of the disease [22]. FP-CIT SPECT is sensitive even in unilateral Parkinson's disease [23]. For studies that focus on pre-symptomatic cases of neurodegenerative diseases like Parkinson's disease, accurate quantitative assessment of BP would be of great interest for detection of preclinical cases, for a better understanding of the degenerative process and for evaluation of neuroprotective treatments. However, the importance of accurate quantitative assessment of BP in this situation has not been studied.

The purpose of this study was to assess the impact of PVE correction on the differential diagnosis between DLB and AD during life. We studied the value of sophisticated data processing for quantitative analysis of clinical trial data involving 23 patients with a high diagnostic probability of DLB or AD. Furthermore, we tested the quantification method in realistic simulated cases mimicking pre-symptomatic stages of DLB for which recruitment and diagnosis are more challenging.

Materials and methods

Patients

Twenty-three patients suffering from DLB or AD were studied. The inclusion criteria were age older than 50 years, consultation for a neuropsychological evaluation with diagnostic criteria of primary degenerative disease using the International Classification of Diseases (ICD-10) and a score of between 16 and 24 on the Mini-Mental State Examination (MMSE). The study protocol was approved by the local ethics committee. All patients gave informed and written consent. Diagnosis of AD was established using the DSM IV criteria, and that of DLB using international consensus criteria [8]. Only patients with probable DLB and AD were included. These inclusion criteria excluded patients suffering from an early form of DLB or AD. Ten patients were diagnosed as having DLB (one woman, nine men, mean age 74 years; mean MMSE 19.7) and 13 as having AD (seven women, six men, mean age 74 years; mean MMSE 20.9) (Table 1). Before tracer injection, 400 mg of potassium perchlorate was orally administered to prevent from radioiodine uptake by the thyroid. All patients were intravenously injected 4 h prior to examination with 185 MBq of ^{123}I-FP-CIT (DaTSCAN; Amersham Health).

Beside these patient populations, two simulated data sets were generated. A Monte Carlo simulation of the SPECT scan of each AD and DLB patient was performed, in order to obtain clinical-like data for which all characteristics were known.

To test our quantification approach on a controlled population of pre-symptomatic patients who cannot be recruited in practice, we also simulated 17 patients corresponding to pre-symptomatic DLB (see below).

SPECT acquisitions

SPECT studies were acquired on a three-headed PRISM 3000 XP camera (Philips) using high-resolution, low-energy fan-beam collimators. The camera was equipped with a fillable line transmission source, located at the focal length (50 cm) of the collimator opposite to one head. System spatial resolution described by the full-width at half-maximum (FWHM) in the "object plane" at a distance equal to the radius of rotation of 15.9 cm was 11 mm. The transmission source was filled with 111 MBq/ml of ^{99m}Tc. For all tomographic acquisitions, 120 projections (step and shoot mode, matrix size 128×128, pixel size 2.1 mm) were acquired over 360°. Three datasets were obtained:

1. A 300-s blank scan was performed in the 20% energy window centered on 140 keV (126–154 keV). The blank scan included about 14 million counts in the whole field of view.
2. With the patient lying on the table with the brain centered in the field of view, an emission scan (E) was acquired (45 s/projection) in four energy windows (92–139 keV, 139–142 keV, 142–175 keV and 175–179 keV). This acquisition yielded about 3.5 million counts in the set of projections corresponding to the 142–175 keV energy window.
3. Without moving the patient, a transmission scan (T) (7.5 s/projection) was acquired in the 20% energy window centered on 140 keV (126–154 keV). This acquisition yielded about 53 million counts between 126 and 154 keV.

The total duration of the examination was 50 min per patient.

MRI acquisitions

Each patient underwent an MRI acquisition on a GEMS system (1.5 Tesla) 1 week before the SPECT acquisition. A 3D echo-gradient sequence was used (TR 5,000 ms, TE 105 ms). The MRI slices were 2 mm thick with a pixel size of 1 mm (matrix size 256×256). Total scan time was 4 min. For each patient, MRI volume was resampled in

Table 1. DLB and AD patient characteristics (mean±1 standard deviation)

	Age (yr)	Sex	MMSE score	Brain volume (ml)	Putamen volume (ml)	Caudate volume (ml)
DLB	73.6±9.5	9M, 1F	19.7±2.6	1,428.4±153.8	4.4±0.6	3.0±0.3
AD	74.5±7.7	6M, 7F	20.9±2.7	1,346.3±145.9	4.4±0.6	2.9±0.6

3.6-mm-thick slices. The two caudate nuclei, two putamen, brain contours, skull and conjunctive tissues were manually segmented on the resampled MR images.

Monte Carlo simulations

Patient simulations

For each patient identified as having AD or DLB, a Monte Carlo simulation of the FP-CIT scan was performed using the SimSET code [24]. The anatomical data needed for the simulations were derived from the segmented MRI scan of the patient. [123]I activity concentrations equal to those found from the patient SPECT data after all corrections, using a calibration coefficient as described below, were set in five compartments: left and right caudate nuclei, left and right putamen and rest of the brain. The simulated value of BP averaged over the left and right structures in the caudate nuclei ranged from 7.0 to 14.8 (mean 10.1±2.3) for AD patients and from 1.8 to 7.6 (mean 5.1±2.2) for DLB patients. The simulated BP value in the putamen ranged from 6.5 to 11.1 (mean 8.6±1.5) for AD patients and from 1.2 to 2.8 (mean 1.9±0.5) for DLB patients. The segmented MRI was also used to derive the attenuation map required for the simulation, by setting appropriate attenuation coefficients at 159 keV to air (0 cm^{-1}), brain tissue (0.15 cm^{-1}), connective tissue (0.17 cm^{-1}) and skull (0.31 cm^{-1}).

The Monte Carlo simulation modelled the effects of attenuation and Compton and Rayleigh scatter. Distance-dependent fan-beam collimator response was modelled analytically (no transport of photons in the collimator was simulated) using an analytical model of the collimator response function given the characteristics of the fan-beam collimators. The response of the photomultiplier tubes and associated electronics was modelled by convolving the simulated projections by a 2D Gaussian function. The imaging system FWHM in the "object plane" at a distance corresponding to the 15.9-cm radius of rotation was 7 mm.

One hundred and twenty emission projections (128×128 matrix) were obtained over 360° with a pixel size of 2.1 mm for each of 16 energy windows (4.75 keV wide) from 102 keV to 178 keV. Around two hundred million photons were generated and 3.5 million events were detected in the projections corresponding to the 20% energy window centered on 159 keV.

Simulations of pre-symptomatic DLB patients

Simulations of patients corresponding to pre-symptomatic DLB patients were also performed with SimSET, using the same approach as for the simulations of real patients. These simulations used brain anatomy derived from the real patient MRI but uptake values mimicking pre-symptomatic disease. These values were chosen so as to be greater than those observed in our probable DLB patients but smaller than those observed in the AD patients. The simulated value of BP for pre-symptomatic DLB patients averaged over the left and right structures ranged from 4.3 to 6.3 (mean 5.6±0.6) in the putamen and from 6.6 to 8.9 (mean 7.6±0.5) in the caudate nuclei.

SPECT data processing and reconstruction

Four processing schemes were considered:

– No correction (NC): 20% energy window projections reconstructed without any correction
– AC: projections reconstructed with attenuation correction

– SAC: projections corrected for scatter and reconstructed with attenuation correction
– SAC-PVC: scatter corrected projections reconstructed using attenuation correction and then corrected for PVE

Scatter correction

Scatter correction was performed using the triple energy window (TEW) method [25], considering the 142–174 keV window as the principal window and the 139–142 keV and 174–179 keV windows as secondary energy windows. In addition, for Monte Carlo simulations, projections including primary events only were considered to assess the results that could be obtained when using an "ideal" scatter correction.

Attenuation correction

Attenuation was corrected for by modelling attenuation in the ordered subset expectation maximisation (OSEM) [26] reconstruction algorithm. For the simulated data, the attenuation map used to perform the simulations was considered for attenuation correction. For the acquired data, the transmission projections were first corrected for emission contamination using the method described by Tung et al. [27]. These corrected transmission data were converted into projections of linear attenuation coefficients, then reconstructed using OSEM (12 iterations, 12 subsets) and convolved by a 3D Gaussian filter of 4 mm FWHM. The resulting transmission maps were linearly scaled from 140 keV to 159 keV to get the attenuation coefficients appropriate for ^{123}I emission data.

Reconstruction

The simulated and acquired projections were reconstructed using OSEM involving a fan-beam projector [26] with 12 iterations and 12 subsets to ensure convergence. Reconstructed images were then convolved by a 3D Gaussian filter of 8.5 mm FWHM. The reconstructed pixel size was 2.1 mm with a slice thickness of 3.6 mm.

Partial volume effect correction

For the patient data, the reconstructed SAC SPECT images were registered with the MRI data using a rigid transformation maximising mutual information [28] (Pixies software, Apteryx, France, http://imaging.apteryx.fr/pixies). The three translation and three rotation parameters were applied to all reconstructed SPECT images (NC, AC, SAC). The segmented MR images of the patients were used to define the left and right caudate nuclei, left and right putamen and rest of the brain. A constant activity concentration A_i was assumed in each of these five compartments.

Correction for PVE was performed by estimating the contamination between compartments [29]. The method expresses the mean value measured in compartment C_j as the weighted sum of the activity concentration A_i present in each compartment i:

$$C_j = \sum_i W_{ij} A_i, \qquad (1)$$

where W_{ij} represents the contribution of compartment i to activity measured in compartment j. Using this model, the activity concentration A_i in each compartment can be estimated by inverting Eq. 1 given the measured activity values C_j in the different compartments and the weights W_{ij}. For each compartment, a volume of images with 1 in the compartment and 0 outside was analytically projected using a

fan-beam projector and modelling attenuation. To mimic the imaging system response function, the resulting projections were convolved by a 2D Gaussian function of 7 mm FWHM for the Monte Carlo simulations and 11 mm FWHM for the acquisitions. The resulting projections were reconstructed and filtered using the same protocols as for the real data. For each compartment i, the value in C_j in the resulting reconstructed images divided by the number of pixels in compartment i gave the weight W_{ij}.

Quantitative measurements

Calibration for absolute quantitation

To estimate absolute activity values in patient data, a calibration factor relating a number of detected counts per second in a region to an activity was obtained, as described in [19]. Briefly, a 91-ml ^{123}I sphere SPECT acquisition was performed using the same protocol as was used for the patient scans. The sphere projections were corrected for scatter using the TEW method and scaled to the total number of photons detected between 92 and 175 keV to obtain projections identical to those that would be obtained if all detected photons were unscattered. These rescaled projections were reconstructed with OSEM including attenuation correction. The calibration factor was deduced as the ratio between the known amount of activity in the sphere and the number of counts per second in the whole reconstructed volume. To estimate activity concentrations from patient acquisitions, the scatter-corrected projections were scaled to the total number of counts acquired between 92 and 175 keV. These scaled projections were then reconstructed with attenuation correction and PVE correction. The measured number of counts on the reconstructed images in the five volumes of interest (VOIs) defined on the patient MR images were multiplied by the calibration factor to obtain the activity in these regions. These activity values were used to perform the Monte Carlo simulations corresponding to the patient data.

Assessment of quantitative accuracy

For the simulated data, mean striatal activity was measured in the putamen and caudate nucleus regions as defined for simulating the activity maps, and mean background brain activity was measured in a 3,500-voxel 3D cylindrical region in the occipital area. For the real data, the striatal VOIs manually defined on MR images and employed for performing the simulations were used. Brain activity was measured in the same cylindrical region as used for the simulations. For each processing scheme, a binding potential value (BP) between striata and brain region was assessed on the reconstructed images, as (striatal activity–background activity)/(background activity) for each of the four striatal VOIs. An asymmetry index (Asym) between left and right structures was calculated for each processing scheme, for caudate and putamen, using:

$$\text{Asym} = 100 \tag{2}$$
$$\times \left[\text{Mean}\left(\text{BP}_{\text{left}}, \text{BP}_{\text{right}}\right) - \text{Min}\left(\text{BP}_{\text{left}}, \text{BP}_{\text{right}}\right) \right]$$
$$/ \text{Mean}\left(\text{BP}_{\text{left}}, \text{BP}_{\text{right}}\right),$$

where Mean(BP$_{\text{left}}$,BP$_{\text{right}}$) is the average BP value over the left and right structures, and Min(BP$_{\text{left}}$,BP$_{\text{right}}$) is the minimum BP value of the left and right structures. Asym was systematically calculated for the caudate nuclei and for the putamen.

For Monte Carlo simulations, for which simulated BP values were known, percent biases in BP estimates were calculated as:

$$\text{Percent bias} = 100 \times |\text{estimated BP} - \text{true BP}|/\text{true BP} \tag{3}$$

Absolute differences between BP estimates and true BP were calculated as:

$$\text{Absolute difference} = |\text{estimated BP} - \text{true BP}|. \tag{4}$$

Statistical analysis

Analysis of variance and bilateral t test (α=0.05) were used to test the significance of differences between the DLB and AD populations, as a function of the processing schemes (NC, AC, SAC, SAC-PVC) and the considered structure (caudate nuclei or putamen). A paired bilateral t test (α=0.05) was used to assess differences between two processing schemes (among NC, AC, SAC, SAC-PVC).

Results

Figure 1 presents typical MR and SPECT images of a DLB and an AD patient. Table 2 summarises the mean and ranges of BP values as a function of the processing scheme for the patient data. For all quantitative schemes, the mean BP values were significantly different (p<0.005) between DLB and AD populations, had the BP been measured in the putamen or in the caudate nuclei. This was observed for the real patient data (Table 2), and also for the corresponding simulated data. The mean BP values were also significantly different (p<0.005) between the simulated pre-symptomatic DLB and simulated AD populations (results not shown).

Patient studies

Striatal volumes

Mean striatal and brain volumes are given in Table 1. The mean volume of caudate nuclei obtained from manual segmentation of the MRI was 2.9±0.6 ml for AD patients and 3.0±0.3 ml for DLB patients. The mean putamen volume was 4.4±0.6 ml for AD patients and 4.4±0.6 ml for DLB patients. The mean brain volume was 1,346.3±145.9 ml for AD patients and 1,428.4±153.8 ml for DLB patients. There was no significant difference between the mean striatal volumes of DLB and AD patient (bilateral t test, α=0.05). The two groups of patients did not differ significantly in their total brain volume either (bilateral t test, α=0.05).

Impact of the processing scheme on the BP estimates

Without any correction, the mean BP calculated over all patients was 1.2±0.5 for the caudate nuclei and 1.2±0.6 for the putamen. Attenuation correction alone significantly increased BP values: mean BP was 1.4±0.5 (p<0.05) for

Fig. 1. Example of MRI and corresponding SAC SPECT slice for a DLB patient (*1st row*) and an AD patient (*2nd row*). The *last column* presents an image fusion between a SPECT slice and the corresponding MRI slice
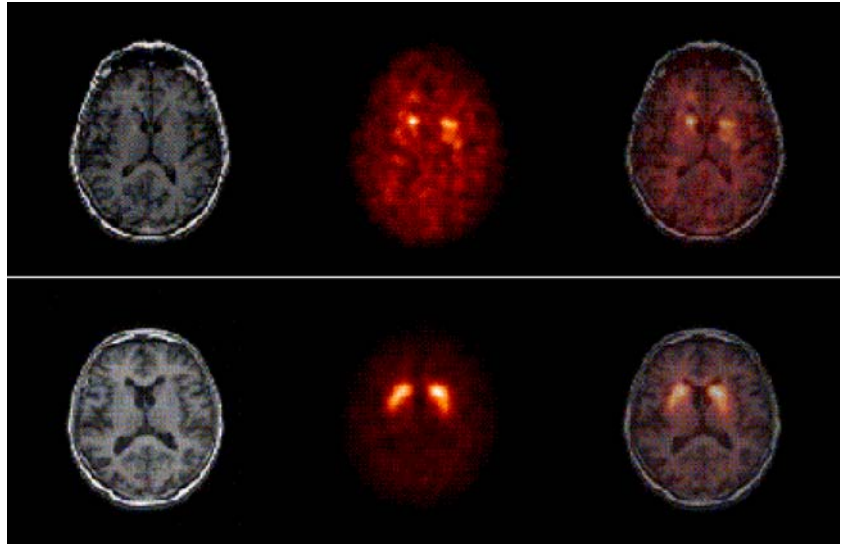
the caudate nuclei and 1.4±0.7 ($p<0.05$) for the putamen. Combining scatter correction with attenuation correction significantly increased the mean BP to 2.1±0.8 ($p<0.05$) for the caudate nuclei and 2.0±1.1 ($p<0.05$) for the putamen. For these three correction schemes (NC, AC, SAC), there was no significant difference between mean BP calculated over the caudate nuclei and mean BP calculated over the putamen (paired bilateral t test, $\alpha=0.05$).

PVE correction introduced the largest changes in BP estimates. Combined with scatter and attenuation corrections, it greatly increased BP to 7.9±3.4 for the caudate nuclei and 5.7±3.6 for the putamen. Unlike what was observed without PVE correction, BP values were significantly greater for the caudate nuclei than for the putamen ($p<0.05$) owing to differences in shape and size between these two structures that induce a greater activity enhancement in caudate nuclei. Indeed, as caudate nuclei were smaller and less compact than putamen, they should be more affected by PVE than putamen for a fixed BP. Biases introduced by PVE also depend on the unknown true BP value: the greater the true BP, the greater the PVE effect. As true BP values were greater for caudate nuclei

than for putamen, biases introduced by PVE were higher for caudate nuclei than for putamen.

Comparison of left and right BP

Table 3 presents the asymmetry index as a function of processing schemes. For each processing scheme, the asymmetry of putamen BP was significantly ($p<0.05$) greater for DLB than for AD patients. For instance, with attenuation and scatter corrections, the asymmetry of putamen BP averaged over patients was 18.3±13.9 for DLB and 6.7±6.3 for AD ($p<0.05$). Whatever the processing scheme, the asymmetry of caudate nucleus BP was not significantly different for DLB and AD patients (bilateral t test). For instance, with attenuation and scatter corrections, the asymmetry of caudate nucleus BP averaged over patients was 12.7±13.1 for DLB and 7.8±8.7 for AD.

For both putamen and caudate structures, the asymmetry index increased significantly when PVE correction was combined with attenuation and scatter corrections ($p<0.05$).

Table 2. Mean BP (±1 standard deviation) and ranges (in parentheses) of the BP estimates in the putamen and caudate nuclei for the patient acquisitions

Corrections	DLB		AD	
	Putamen	Caudate nuclei	Putamen	Caudate nuclei
NC	0.5±0.1	0.7±0.3	1.7±0.2	1.6±0.2
	(0.3–0.7)	(0.3–1.0)	(1.4–2.0)	(1.2–1.9)
AC	0.6±0.1	0.9±0.3	1.9±0.3	1.8±0.3
	(0.4–0.9)	(0.5–1.2)	(1.6–2.4)	(1.4–2.1)
SAC	0.9±0.2	1.3±0.5	2.9±0.4	2.7±0.4
	(0.5–1.2)	(0.6–1.9)	(2.3–3.5)	(1.9–3.2)
SAC-PVC	1.9±0.5	5.1±2.2	8.6±1.5	10.1±2.3
	(1.2–2.8)	(1.8–7.6)	(6.5–11.1)	(7.0–14.8)

Table 3. Mean asymmetry index (±1 standard deviation) in the putamen and caudate nuclei for patient acquisitions

	DLB		AD	
	Putamen	Caudate nuclei	Putamen	Caudate nuclei
BP_{NC}	17.3±12.7	13.9±10.8	7.0±4.9	7.7±7.6
BP_{AC}	14.2±8.8	11.0±9.4	6.7±5.3	7.3±8.5
BP_{SAC}	18.3±13.9	12.7±13.1	6.7±6.3	7.8±8.7
$BP_{SAC-PVC}$	29.2±19.8	12.4±12.3	12.3±11.9	15.2±14.9

With all corrections, mean asymmetry indices in putamen were 29.2±19.8 for DLB and 12.3±11.9 for AD.

Impact of the corrections on patient classification

Figures 2 and 3 show the distribution of mean BP in the putamen and in the caudate nuclei respectively, for the four processing schemes, for patients identified as having DLB or AD.

Without any correction, the DLB group showed significantly lower BP than the AD group in all striatal areas: the mean caudate BP was 1.6±0.2 for AD patients and 0.7±0.3 for DLB patients ($p<0.05$), while the mean putamen BP was 1.7±0.2 for AD patients and 0.5±0.1 for DLB patients ($p<0.05$). The two populations could be perfectly distinguished based on the caudate or putamen BP (Figs. 2 and 3 and the range of BP values in Table 2). The separation between the two populations was clearer when considering BP measured in the putamen than when considering BP measured in the caudate nuclei. For the AD patients, there was no significant difference between the mean BP calculated over the caudate nuclei and the mean BP calculated over the putamen. For DLB patients, BP in caudate nuclei was significantly greater than BP in putamen ($p<0.05$).

Similar to what was observed without any correction, when using attenuation correction only, the AD and DLB groups were clearly separated based on the BP values. Mean BP in the caudate nuclei was 1.8±0.3 for AD patients and 0.9±0.3 for DLB patients ($p<0.05$) and mean putamen BP was 1.9±0.3 for AD patients and 0.6±0.1 for DLB patients ($p<0.05$). Again, the separation between the two pathologies was clearer when considering the putamen BP than the caudate nuclei BP. For AD patients, there was no significant difference between caudate nuclei and putamen BP. For DLB patients, BP in caudate nuclei was significantly greater than BP in putamen ($p<0.05$).

When considering the processing scheme involving attenuation and scatter corrections, the AD and DLB groups were also clearly distinct based on the BP values in putamen, but not in caudate nuclei (Figs. 2 and 3). Mean BP in the caudate nuclei was 2.7±0.4 for AD patients and 1.3±0.5 for DLB patients ($p<0.05$) and mean putamen BP was 2.9±0.4 for AD patients and 0.9±0.2 for DLB patients ($p<0.05$). A threshold BP value separated the two groups only when considering putamen BP. There was a significant difference between BP calculated over the caudate nuclei and BP calculated over the putamen only for the DLB patients ($p<0.05$).

When combining PVE correction with attenuation and scatter corrections, mean BP in caudate nuclei was 10.1±2.3 for AD patients and 5.1±2.2 for DLB patients ($p<0.05$). Mean BP in putamen was 8.6±1.5 for AD patients and 1.9±0.5 for DLB patients ($p<0.05$). When considering BP values in caudate nuclei, the AD and DLB groups overlapped. As overlap was also observed without PVE correction, this suggests that the BP measured in caudate nuclei is not useful for differential diagnosis between AD and DLB. Conversely, the two groups could be perfectly distinguished based on the putamen BP, without and with PVE correction, suggesting that the BP measured in putamen is helpful for differential

Fig. 2. Distribution of BP averaged over the two putamen for patients clinically identified as having DLB or AD, represented as box and whisker plots with no correction (BP_{NC}), with attenuation correction (BP_{AC}), with attenuation and scatter corrections (BP_{SAC}) and with all corrections ($BP_{SAC-PVC}$). The median (■), the smallest and the greatest values (●), the interquartile range (*box*) and the interdecile range (*whiskers*) of the BP distribution are shown
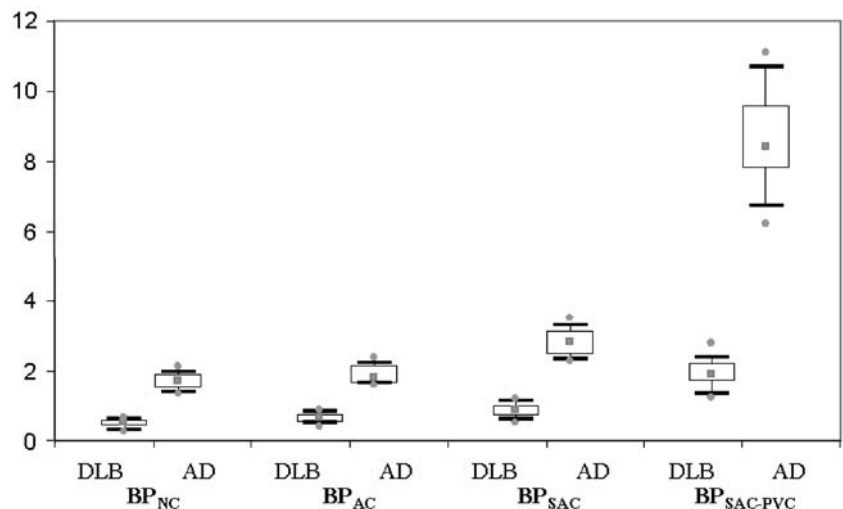
Fig. 3. Distribution of BP averaged over the two caudate nuclei for patients clinically identified as having DLB or AD, represented as box and whisker plots with no correction (BP$_{NC}$), with attenuation correction (BP$_{AC}$), with attenuation and scatter corrections (BP$_{SAC}$) and with all corrections (BP$_{SAC-PVC}$). The median (■), the smallest and the greatest values (●), the interquartile range (*box*) and the interdecile range (*whiskers*) of the BP distribution are shown
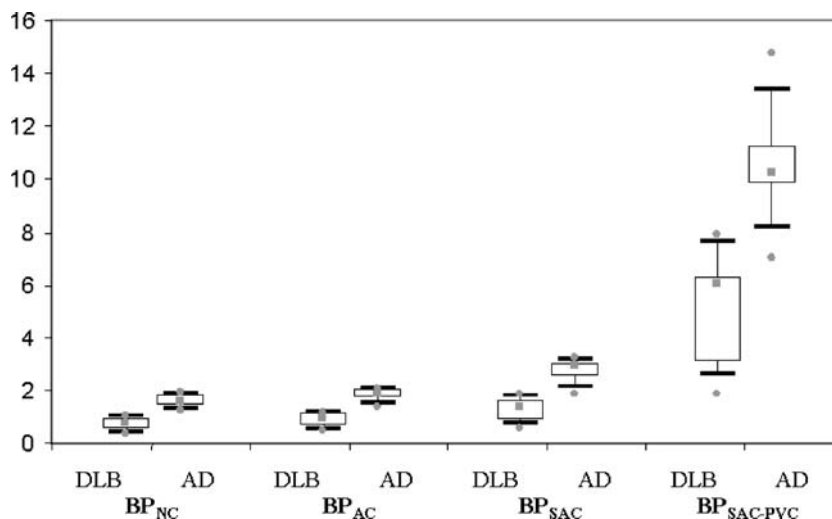
diagnosis between AD and DLB. With PVE correction, there was a significant difference between BP calculated over the caudate nuclei and BP calculated over the putamen only for DLB patients ($p<0.05$).

Comparison between real and simulated patient data

Biases in BP estimates as a function of the processing scheme

Monte Carlo simulations of the 23 patient scans allowed us to objectively assess the quantitative accuracy in BP estimates achieved using different processing protocols. In the simulated patients, without any correction, BP was underestimated by 78.1% on average in the caudate nuclei and by 66.4% on average in the putamen (Table 4). After attenuation correction only, BP was underestimated by 74.5% on average in the caudate nuclei and by 59.7% in the putamen. After attenuation and TEW corrections, BP was underestimated by 71.3% on average in the caudate nuclei and by 55.1% in the putamen. The average absolute difference between true BP and measured BP was 5.7 in the caudate nuclei and 3.6 in the putamen.

Using the projections of primary events as representative of what could be obtained if a perfect scatter correction were available, biases were very close to those obtained with TEW correction, suggesting that TEW correction was reliable enough (Table 4).

Similar to what was observed on the patient data, PVE correction greatly affected BP values. When combined with scatter and attenuation corrections, it yielded an averaged overestimation of BP estimates of 13.4% in the caudate nuclei and of 16.1% in the putamen. The mean absolute difference between true BP and measured BP was then 0.9 in the caudate nuclei and 0.6 in the putamen.

Comparison of BP measured on simulated and acquired data

Without any correction, in the putamen, BP averaged over all real patients was 1.2±0.6, while it was 1.6±0.8 for the corresponding simulated patients. In the caudate nuclei, BP averaged over all real patients was 1.2±0.5, while it was 1.7±0.7 for the corresponding simulated patients. With all corrections, in the putamen, the BP averaged over all real patients was 5.7±3.6, compared with 5.9±3.6 for

Table 4. Mean absolute differences and mean percent biases in BP estimates for the putamen and caudate nuclei in the simulations of patients for which real SPECT scans were obtained

Corrections	Methods	Putamen	Caudate nuclei
NC	20%+OSEM	3.8 (−66.4%)	5.9 (−78.1%)
AC	20%+OSEM-A	3.8 (−59.7%)	5.9 (−74.5%)
SAC	TEW+OSEM-A	3.6 (−55.1%)	5.7 (−71.3%)
SAC	PRIM+OSEM-A	3.7 (−57.3%)	5.7 (−72.4%)
SAC-PVC	TEW+OSEM-A+PVC	0.6 (+16.1%)	0.9 (+13.4%)

OSEM-A OSEM including attenuation correction, *PRIM* projections including primary events
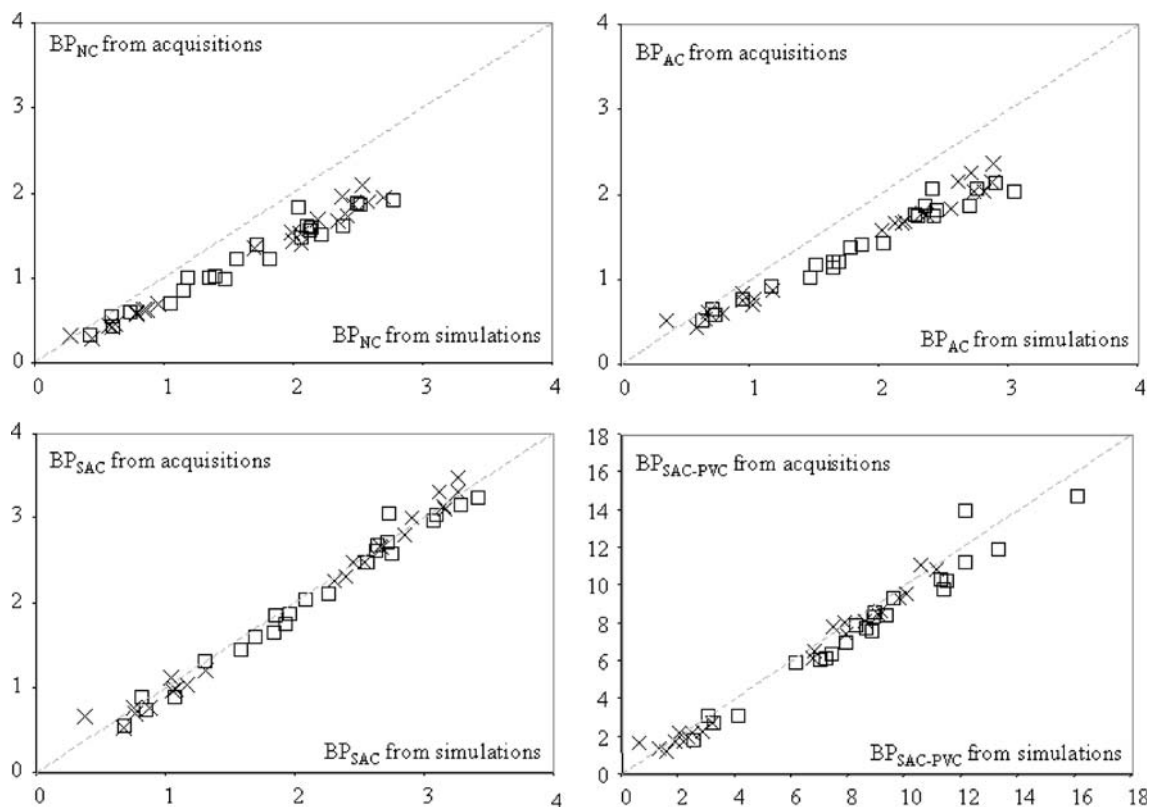
Fig. 4. Mean BP in the putamen measured on the patient data as a function of mean BP in the putamen measured on the corresponding simulated patients. DLB (×) or AD (□) are shown with different symbols. Results are shown for BP estimated with: (**a**) no correction (BP_{NC}), (**b**) attenuation correction (BP_{AC}), (**c**) attenuation and scatter corrections (BP_{SAC}) and (**d**) all corrections ($BP_{SAC-PVC}$)

the corresponding simulated patients. In the caudate nuclei, the BP averaged over all real patients was 7.9± 3.4, compared with 8.6±3.4 for the corresponding simulated patients. Figure 4 shows the BP values measured on the real patient data as a function of the BP values measured on the simulated patient data for the four processing schemes. Without any correction or with attenuation correction only, BP values were higher on simulated data than on real data (see Sect. Discussion). With attenuation and scatter corrections or with all

corrections, BP values measured on simulated data were almost identical to those measured on the corresponding patient data.

Simulations of patients with pre-symptomatic DLB

Real patient data demonstrate that putamen BP best separated DLB from AD patients (see above). Therefore, only results corresponding to putamen BP are presented for

Fig. 5. Distribution of BP averaged over the two putamina for simulated patients assigned as pre-symptomatic DLB or AD represented as box and whisker plots without any correction (BP_{NC}), with attenuation correction (BP_{AC}), with attenuation and scatter corrections (BP_{SAC}), and with all corrections ($BP_{SAC-PVC}$). The median (■), the smallest and the greatest values (●), the interquartile range (*box*) and the interdecile range (*whiskers*) of the BP distribution are shown
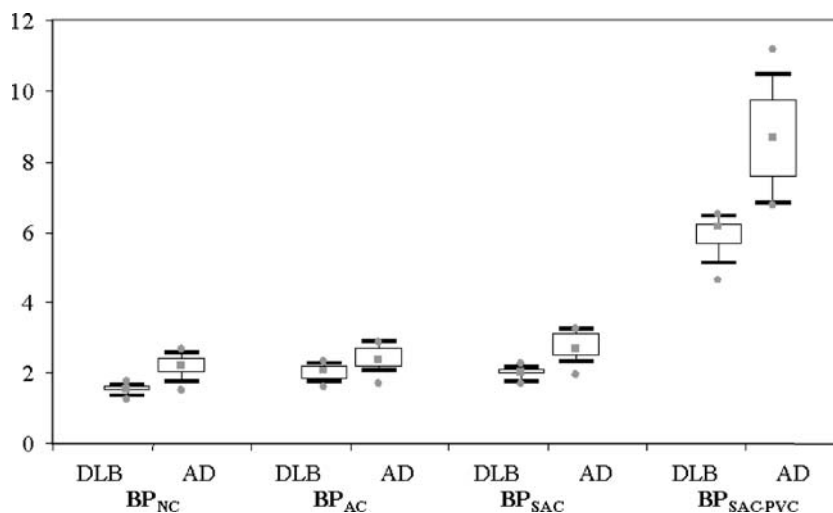
the study concerning the simulations of patients with pre-symptomatic DLB.

In the 17 simulations corresponding to pre-symptomatic DLB patients, the simulated value of putamen BP averaged over the left and right putamen ranged from 4.3 to 6.3 (mean 5.6±0.6) while putamen BP ranged from 6.5 to 11.5 (mean 8.3±2.0) for the 13 simulated AD patients.

Figure 5 shows the putamen BP values as a function of the processing scheme for the simulated patients with pre-symptomatic DLB and for the simulated AD patients. Without any correction, the averaged BP was 2.3±0.3 in the putamen for AD patients and 1.5±0.1 for pre-symptomatic DLB patients ($p<0.05$), with 13 out of 30 patients with BP values in a range where AD and DLB could not be distinguished. With attenuation correction, the averaged BP was 2.5±0.3 in the putamen for AD patients and 2.0±0.2 for pre-symptomatic DLB patients ($p<0.05$), with 22 out of 30 patients with BP values in a range where DLB and AD overlapped. With attenuation and scatter corrections, the averaged BP in the putamen was 2.8±0.3 for AD patients and 2.0±0.1 for pre-symptomatic DLB patients ($p<0.05$), with 15 patients who could not be classified as having DLB or AD based on the BP value. When combining PVE correction with attenuation and scatter corrections, the putamen BP averaged over all patients was 8.9±1.4 for AD patients and 5.9±0.6 for pre-symptomatic DLB patients ($p<0.05$); the two populations could be perfectly distinguished based on the BP values by considering a threshold between 6.5 and 6.8.

Discussion

This study confirms that FP-CIT SPECT can differentiate between DLB and AD. We found that striatal volume variations only did not explain the differences in estimated BP in the AD and DLB groups through PVE (PVE artificially reduces BP more in small structures than in large structures): indeed, neither absolute putamen volume nor absolute caudate nucleus volume was significantly different between AD and DLB patients. This is consistent with the results reported in the literature for absolute volumes [30–33].

We assessed the value and limitations of BP measurements from the SPECT images. We showed that only a complete processing scheme including scatter, attenuation and PVE corrections could accurately estimate BP (Table 4). TEW scatter correction was reliable for our purpose, since, when combined with attenuation correction, it yielded results close to those obtained when considering unscattered events only. The most important correction for accurate estimates of BP is PVE correction. The PVE correction we considered requires the segmentation of brain structures that can present different activity concentrations. This segmentation can be performed from MR images. This PVE correction assumes that the anatomical compartments and the functional compartments share the same boundaries. It also assumes that the dopaminergic transporters are uniformly distributed within each anatomical compartment.

For simulated patients in which PVE correction was not affected by registration or segmentation errors, errors in BP estimates were less than 16% when correcting for scatter, attenuation and PVE. These residual percent errors are actually artificially large because for some simulated DLB patients, true BP (hence the denominator of the percent error) was less than 1. The corresponding mean absolute difference between measured BP and true BP was in fact only 0.6 for putamen and 0.9 for caudate nuclei (Table 4).

In a previous paper [19], we demonstrated that the accuracy of PVE correction strongly depended on the precision of the segmentation of MR images and of the SPECT/MR image registration. For the patients considered in the present study, our results can thus be biased by MRI segmentation errors or by SPECT/MRI registration errors. Monte Carlo simulations allowed us to test our quantification methods while being sure that no segmentation or registration errors occurred. For each patient, if segmentation and registration were correct, then PVE should have induced the same error on simulation as on real data and corrections for attenuation and scatter should have acted similarly for acquired and simulated data. This was actually the case (Fig. 4). However, even if BPs observed on acquired and simulated data were similar, several errors of segmentation and registration may have occurred and compensated each other. Consistency between acquired and simulated results is necessary but not sufficient to prove that no errors have occurred during MRI segmentation or SPECT/MRI registration in patients. Without any correction, BP values were higher for Monte Carlo simulations than for the corresponding acquisitions. This is because our simulations did not model the high-energy emission rays of ^{123}I or the physical interactions of photons with the collimator [19]; hence simulated data included less scattered events than real data. Because scattered events decreased contrast, BP values were higher in simulated data which contained less scattered events when scatter correction was not applied [19]. When TEW correction was applied, scatter from high-energy photons was mostly removed and BP values assessed from real and simulated data became similar.

The considered quantification method based on BP measurement in putamen clearly separated patients clinically diagnosed as having probable DLB or AD both without and with PVE correction. These findings are consistent with previous work in this field, in which no corrections for physical effects were used [10–13, 34]. It is nevertheless difficult to compare BP values obtained in these previous studies with our values because the corrections of the SPECT data and the way BP values were measured were different from those in our approach. We found that the dopamine transporter loss differentiating DLB from AD patients was more pronounced in the putamen than in the caudate nuclei, for all processing schemes, which is consistent with previous findings [10].

We did not show any clinical advantage of using PVE correction for differential diagnosis between AD and DLB. By their nature, clinical trials include only symptomatic patients with already severely reduced dopamine transport-

er levels. Moreover, we included relatively advanced symptomatic stages of DLB (probable DLB). When simulating patients mimicking pre-symptomatic DLB, with BP values in putamen of between 4.3 and 6.3, we showed that PVE correction improved the accuracy of classification of patients. These values are somewhat arbitrary, but this was the only way to test our quantification method on a pre-symptomatic population of such patients. In DLB, there is no possibility of testing the method in "hemi-symptomatic" patients like in hemi-parkinsonism, where the contralateral side provides a model of pre-symptomatic alteration [23].

Figure 5 suggests that, for our acquisition and processing protocols, BP values in putamen of between 1.4 and 1.8 without any correction are the values for which PVE correction would probably be most useful to facilitate patient classification.

Although our study addresses specifically the differential diagnosis between AD and DLB, our results suggest that a comprehensive image processing scheme including scatter, attenuation and PVE corrections might be useful in other neurological applications. For instance, the proposed method might help facilitate the diagnosis of Parkinson's disease at early stages.

For studies focussing on the detection of pre-symptomatic cases of DLB or Parkinson's disease, PVE correction may increase the accuracy with which preclinical cases are detected. Quantitative analysis is important for possible preclinical diagnosis, for a better understanding of disease evolution and for evaluation of neuroprotective treatment.

Conclusion

We previously demonstrated, using simulations and phantom experiments, that when combined with attenuation and scatter corrections, PVE correction was effective at reducing the biases in BP estimates, with errors of about 10% in dopaminergic neurotransmission ^{123}I SPECT imaging. When applying this processing to 23 probable Alzheimer and DLB patients, we found that measurement of putamen BP with or without PVE correction yielded a perfect differentiation between these two pathologies. Using Monte Carlo simulations, we demonstrated that for pre-symptomatic stages of DLB, PVE correction was necessary for accurate differential diagnosis between DLB and AD.

References

1. Marek K, Seibyl J, Zoghbi S. [^{123}I] beta-CIT SPECT imaging demonstrate bilateral loss of dopamine transporters in hemi-Parkinson's diseases. Neurology 1996;46:231–237

2. Booij J, Tissingh G, Boer G, Speelman J, Stoof J, Janssen A, et al. [^{123}I]FP-CIT SPECT shows a pronounced decline of striatal dopamine transporter labelling in early and advanced Parkinson's disease. J Neurol Neurosurg Psychiatry 1997;62:133–140

3. Benamer T, Patterson J, Grosset D, Booij J, de Bruin K, van Royen E, et al. Accurate differentiation of parkinsonism and essential tremor using visual assessment of [^{123}I]-FP-CIT SPECT imaging: the [^{123}I]-FP-CIT study group. Mov Disorder 2000;15:503–510

4. Booij J, Tissingh G, Winogrodzka A, van Royen EA. Imaging of the dopaminergic neurotransmission system using single-photon emission tomography and positron emission tomography in patients with parkinsonism. Eur J Nucl Med 1999;26:171–182

5. Booij J, Speelman JD, Horstink MW, Wolters EC. The clinical benefit of imaging striatal dopamine transporters with ^{123}I-FP-CIT SPET in differentiating patients with presynaptic parkinsonism from those with other forms of parkinsonism. Eur J Nucl Med 2001;28:266–272

6. Tatsch K, Asenbaum S, Bartenstein P, Catafau AM, Halldin C, Pillowsky LS et al. European Association of Nuclear Medicine procedure guidelines for brain neurotransmission SPET using ^{123}I-labelled dopamine D_2 receptor ligands. Eur J Nucl Med Mol Imaging 2002;29:BP23–BP29

7. Tatsch K. Imaging of the dopaminergic system in parkinsonism with SPET. Nucl Med Commun 2001;22:819–827

8. McKeith IG, Galasko D, Kosaka K, Perry EK, Dickson DW, Hansen LA et al. Consensus guidelines for the clinical and pathologic diagnosis of dementia with Lewy bodies (DLB): report of the consortium on DLB international workshop. Neurology 1996;47:1113–1124

9. McKeith LG, Ballard CG, Perry RH, Ince PG, O'Brien JT, Neill D et al. Prospective validation of consensus criteria for the diagnosis of dementia with Lewy bodies. Neurology 2000;54:1050–1058

10. O'Brien JT, Colloby S, Fenwick J, Williams ED, Firbank M, Burn D et al. Dopamine transporter loss visualized with FP-CIT SPECT in the differential diagnosis of dementia with Lewy bodies. Arch Neurol 2004;61:919–925

11. Walker Z, Costa DC, Walker RW, Shaw K, Gacinovic S, Stevens T et al. Differentiation of dementia with Lewy bodies from Alzheimer's disease using a dopaminergic presynaptic ligand. J Neurol Neurosurg Psychiatry 2002;73:134–140

12. Walker Z, Costa DC, Walker RW, Lee L, Livingston G, Jaros E et al. Striatal dopamine transporter in dementia with Lewy bodies and Parkinson disease: a comparison. Neurology 2004;62:1568–1572

13. Costa DC, Walker Z, Walker RW, Fontes FR. Dementia with Lewy bodies versus Alzheimer's disease: role of dopamine transporter imaging. Mov Disorder 2003;18:S34–S38

14. Tatsch K, Asenbaum S, Bartenstein P, Catafau AM, Halldin C, Pillowsky LS et al. European Association of Nuclear Medicine procedure guidelines for brain neurotransmission SPET using ^{123}I-labelled dopamine D_2 transporter ligands. Eur J Nucl Med Mol Imaging 2002;29:BP30–BP35

15. Chouker M, Tatsch K, Linke R, Pogarell O, Hahn K, Schwarz J. Striatal dopamine transporter binding in early to moderate advanced Parkinson's disease: monitoring of disease progression over 2 years. Nucl Med Commun 2001;22:721–725

16. Marek K, Seibyl J, Shoulson I. Dopamine transporter brain imaging to assess the effects of Pramipexole vs levodopa on Parkinson disease progression. JAMA 2002;287:1653–1661

17. Hashimoto J, Sasaki T, Ogawa K, Kubo A, Motomura N, Ichihara T et al. Effects of scatter and attenuation correction on quantitative analysis of beta-CIT brain SPET. Nucl Med Commun 1999;20:159–165

18. Almeida P, Ribeiro MJ, Bottlaender M, Loc'h C, Langer O, Strul D et al. Absolute quantitation of iodine-123 epidepride kinetics using single-photon emission tomography: comparison with carbon-11 epidepride and positron emission tomography. Eur J Nucl Med 1999;26:1580–1588

19. Soret M, Koulibaly PM, Darcourt J, Hapdey S, Buvat I. Quantitative accuracy of dopaminergic neurotransmission imaging with ^{123}I SPECT. J Nucl Med 2003;44:1184–1193

20. Hoffman EJ, Huang SC, Phelps ME. Quantitation in positron emission computed tomography: 1. Effect of object size. J Comput Assist Tomogr 1979;3:299–308

21. Bernheimer H, Birkmayer W, Hornykiewicz O, Jellinger K, Seitelberger F. Brain dopamine and the syndromes of Parkinson and Huntington. Clinical, morphological and neurochemical correlations. J Neurol Sci 1973;20:415–455

22. Prunier C, Bezard E, Montharu J, Mantzarides M, Besnard J-C, Baulieu J-L, et al. Presymptomatic diagnosis of experimental Parkinsonism with ^{123}I-PE2I SPECT. Neuroimage 2003;19:810–816

23. Tissingh G, Booij J, Bergmans P, Winogrodzka A, Janssen AG, van Royen E et al. Iodine-123-N-omega-fluoropropyl-2beta-carbomethoxy-3beta-(4-iodophenyl)tropane SPECT in healthy controls and early-stage, drug naive Parkinson's disease. J Nucl Med 1998;39:1143–1148

24. Harisson RL, Haynor DR, Gillispie SB, Vannoy SD, Kaplan MS, Lewellen TK. A public-domain simulation system for emission tomography: photon tracking throught heterogeneous attenuation using importance sampling. J Nucl Med 1993;34:60P

25. Ogawa K, Harata Y, Ichihara T, Kubo A, Hashimoto N. A practical method for position-dependent Compton-scattered correction in single photon emission. IEEE Trans Med Imaging 1991;10:408–412

26. Hudson HM, Larkin RS. Accelerated image reconstruction using ordered subsets of projection data. IEEE Trans Med Imaging 1994;13:601–609

27. Tung c-H, Gullberg GT, Zeng GL, Christian PE, Datz FL, Morgan HT. Non-uniform attenuation correction using simultaneous transmission and emission converging tomography. IEEE Trans Nucl Sci 1992;39:1134–1143

28. Maes F, Collignon A, Vandermeulen D, Marchal G, Suetens P. Multimodality image registration by maximization of mutual information. IEEE Trans Med Imaging 1997;16:187–198

29. Rousset OG, Ma Y, Evans AC. Correction for partial volume effects in PET: principle and validation. J Nucl Med 1998;39:904–911

30. Barber R, McKeith I, Ballard C, O'Brien J. Volumetric MRI study of the caudate nucleus in patients with dementia with Lewy bodies, Alzheimer's disease, and vascular dementia. J Neurol Neurosurg Psychiatry 2002;72:406–407

31. Almeida OP, Burton EJ, McKeith I, Gholkar A, Burn D, O'Brien J. MRI study of caudate nucleus volume in Parkinson's disease with and without dementia with Lewy bodies and Alzheimer's disease. Dement Geriatr Cogn Disord 2003;16:57–63

32. Burton EJ, Karas G, Paling SM, Barber R, Williams ED, Ballard C et al. Patterns of cerebral atrophy in dementia with Lewy bodies using voxel-based morphometry. Neuroimage 2002;17:618–630

33. Cousins DA, Burton EJ, Burn D, Gholkar A, McKeith I, O'Brien J. Atrophy of the putamen in dementia with Lewy bodies but not Alzheimer's disease: an MRI study. Neurology 2003;61:1191–1195

34. Donnemiller E, Heilmann J, Wenning GK, Berger W, Decristoforo C, Moncayo R et al. Brain perfusion scintigraphy with ^{99m}Tc-HMPAO or ^{99m}Tc-ECD and ^{123}I-beta-CIT single-photon emission tomography in dementia of the Alzheimer-type and diffuse Lewy body disease. Eur J Nucl Med 1997;24:320–325